

Anti-amyloidogenic Effects of Polyphenols on Bovine Gamma Globulin and Hen Egg White Lysozyme using Thioflavin-T Fluorescence and Circular Dichroism Spectrometry

Samantha Skaar and Dr. Myoung E. Lee

Department of Chemistry, Winona State University, Winona, Minnesota

ABSTRACT

Alzheimer's disease (AD) is an age-linked disease which involves cognitive impairment as a result of neurodegeneration. The formation of beta-amyloid fibrils in between neurons is a major mechanism contributing to this disease pathology. The formation and degradation of these proteins have been a major target in research for this debilitating disease. Natural compounds have been shown to have anti-amyloidogenic properties and have gained popularity within certain niches. The following natural compounds were added during *in vitro* amyloidogenesis, using bovine gamma globulin (GG) and hen egg white lysozyme (HEWL) as a model system: Epigallocatechin-3-gallate (EGCG), a bioactive compound found in green tea extract; nordihydroguaiaric acid (NDGA), an antioxidant found in the creosote bush; phloretin (PHL), an antioxidant flavonoid in apples; and ellagic acid (EA), a polyphenol and a natural dimeric derivative of gallic acid that is found in fruits and nuts like grapes, strawberries, raspberries, and walnut. Incubation of these solutions and fluorescence analysis using thioflavin-T (ThT) fluorescence revealed a linear dose-dependent response for EGCG when fluorescence was plotted against concentrations of 0, 1, 2, 5, and 10 mM EGCG in HEWL and a hyperbolic dose-dependent response for GG. The coefficient of determination for 1 mg/mL and 2 mg/mL HEWL with EGCG, respectively was 0.9745 and 0.9679. The excitation wavelength used was 440 nm with an emission wavelength of 480 nm. In 2 mg/mL GG, percent activation for 1, 2, 5, and 10 mM EGCG when compared to the control (0 mM) was 114, 186, 990, and 420%, respectively. For 2 mg/mL HEWL, percent activation for 1, 2, 5, and 10 mM EGCG when compared to the control (0 mM) was 117, 134, 221, and 450%, respectively. Fluorescence was also noted to be less for HEWL than for GG as the average fluorescence for the first two hours of analysis for the control 2 mg/mL HEWL was 33.23 and was 989.52 for 2 mg/mL GG under the same conditions. No relationships were observed for NDGA, PHL, and EA. Circular dichroism (CD) data was used to show the composition of secondary structure in GG and HEWL. Both of these proteins with inhibitors of PHL and EA indicated that most of GG's secondary structure has changed to random coil structure and most of HEWL's secondary structure has remained alpha-helical. The presence of PHL and EA during incubation did not affect the secondary structure of GG and HEWL. There is no available CD data for EGCG and NDGA due to time constraints, but may be explored in the future.

INTRODUCTION

The formation of beta-amyloid fibrils within the human brain has been of interest as their characterization has been seen to contribute to diseases such as Parkinson's and Alzheimer's Disease (AD). Formation starts with monomers which then aggregate to form an oligomeric intermediate. Mature fibrils form when these intermediates conjugate.¹ These fibrils are insoluble fibrillary polypeptide aggregates predominantly composed of β -sheet structure in a characteristic cross- β conformation.^{2,3} These mature fibrils comprised of beta-sheet protein structure have a stronger tendency to stack upon one another and aggregate. The kinetic networks of the fibrils are continually being produced and undergo fibrinolysis, however, when the balance is lost, the fibrils are deposited extracellularly and neurodegenerative diseases such as AD—the most common form of dementia—can develop.⁴ Fibrils aggregating between neurons interfere with neural signaling and communication which leads to the symptoms seen in AD such as memory loss and confusion. Because of the prevalence of diseases caused by beta-amyloid fibrils, inhibiting the formation of these disease causing proteins has gained popularity. Finding natural inhibitors of fibril formation has appealed to the general population as they can be proactive in preventing a potential disease and it can be more appealing than other pharmacologic interventions. Naturally occurring polyphenols can aid in anti-amyloidogenic drug design because they are known for their antioxidant and anti-inflammatory properties and they possess a variety of structural backbones. In this study, beta-amyloid fibrils formed using bovine gamma globulin (GG) and hen egg white lysozyme (HEWL) *in vitro* were subjected to different concentrations of four common polyphenols—epigallocatechin-3-gallate (EGCG), nordihydroguaiaric acid (NDGA), phloretin (PHL), and ellagic acid (EA). EGCG (Figure 1) is a naturally occurring polyphenol found in green tea. Along with its antioxidant properties, EGCG has anti-aggregation properties which inhibit the formation of beta-amyloid fibrils. The formation of covalent adducts when nucleophilic thiol/amino groups bind to electrophilic carbonyl groups also affects the binding affinity of EGCG to the fibril.⁵ Additionally, non-covalent interactions allows EGCG to bind directly to the fibril and remodel previously existing fibrils into less toxic insoluble aggregates and prevent the formation of toxic oligomers.^{6,7} Hydrophobic and hydrogen bonding interactions mediate this activity. NDGA (Figure 2) is an antioxidant produced as the main metabolite of the creosote bush. This polyphenol has similar mechanisms to EGCG in binding the pre-formed fibril and contribute to its degradation. A study by Ono and colleagues demonstrated that NDGA inhibited beta-amyloid fibril formation from APP (1-40) and APP (1-42) and it destabilized pre-formed fibrils dose-dependently.⁸ A suggested mechanism for this involves the binding of NDGA's two ortho-dihydroxybenzene rings to free fibrils and preventing their aggregation. The structure could also be suitable for the breakdown of beta-sheets. PHL (Figure 3) is a polyphenol mainly found in apples and strawberries. Among its antioxidant properties, PHL has also been shown to inhibit fibril formation by decreasing the association of beta-amyloid peptides to the membrane. Studies have shown that beta-sheet structures are more prevalent in the presence of negatively charged lipid vesicles.^{9,10} PHL is lipophilic and dipolar so it decreases the membrane dipole potential. Thus, the negative charge of the lipid membrane is decreased and will therefore decrease the association of beta-amyloid peptides.¹¹ EA (Figure 4) is a polyphenol and a natural dimeric derivative of gallic acid that is found in fruits and nuts like grapes, strawberries, raspberries, pomegranate, and walnut. Along with its antioxidant properties, EA has been shown to inhibit fibril formation by interfering with the fibril formation pathway. One study demonstrated that EA inhibited neuronal death and beta-amyloid formation on APP/PS1 mice, which are mice that experience pathological similarities with patients that experience AD.¹² Another study found that EA reduced the presence of inflammatory cytokines produced by NF- κ B and TLR signaling pathways what the presence of beta-amyloid fibrils exacerbate.¹³

The beta-amyloid fibrils formed with GG and HEWL combined with the four aforementioned natural inhibitors were characterized by thioflavin T (ThT) fluorescence and circular dichroism (CD) spectrometry. ThT will only fluoresce when bound to beta-amyloid structures, not when bound to monomers or oligomeric intermediates. This will signify that there are beta-fibrils formed in the controls. When ThT binds the beta sheet, it restrict the bond rotation between the benzothiazole ring and aminobenzene ring. This results in an excitation at 440 nm and emission at 480 nm.¹⁴ (Figure 5) CD spectrometry is commonly used to study the secondary structure of a protein due to the difference in the absorbance of circular polarized lights. In essence, it is the differential absorption of left-handed and right-handed light. Two possible spin angular momentum states are represented by the polarized light which can therefore determine presence of ordered peptide bonds in the protein secondary structure results in a distinct CD spectrum. Alpha helices have three CD bands—one positive and two negative. Beta sheets exhibit two CD bands—one positive and one negative. Lastly, random coils have a strong negative CD band and a weaker positive CD band. Each band is expressed in a specific wavelength alpha-helix shows two negative bands at 222 nm and 208 nm. Beta-sheet shows one negative band at 218 nm. The random coil structure shows a negative band at 195 nm (Figure 6).

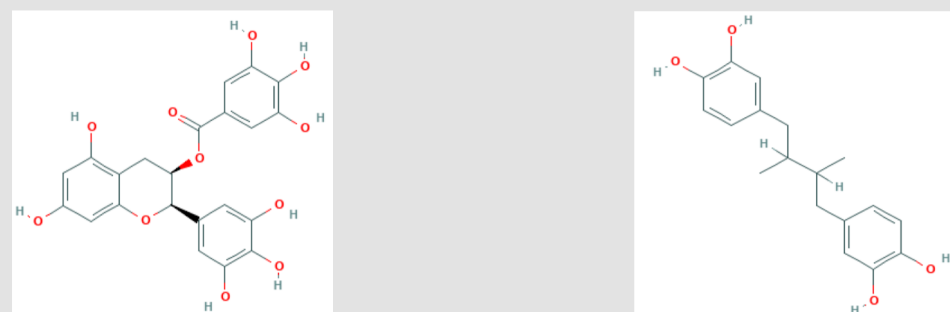


Figure 1: Structure of EGCG

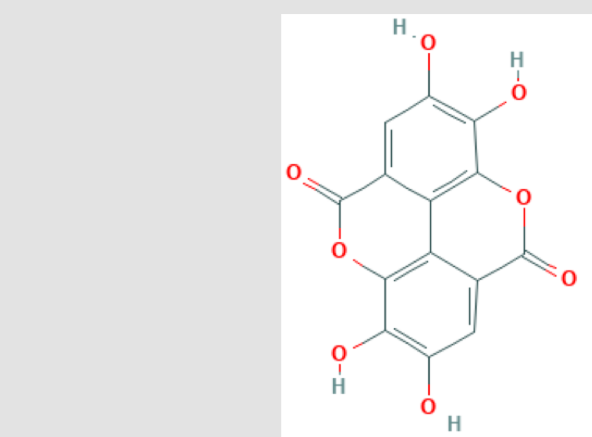


Figure 4: Structure of EA

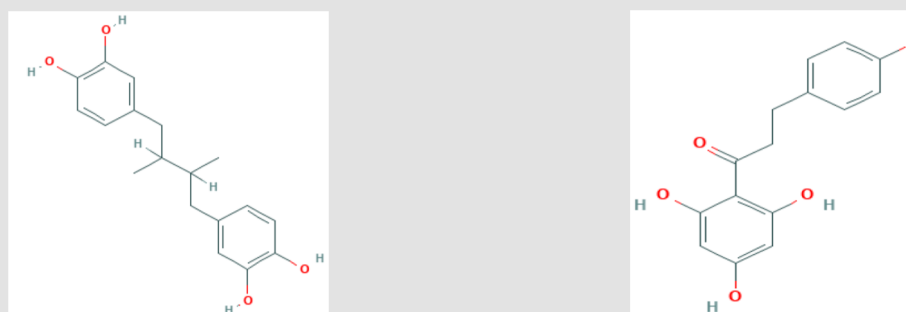


Figure 2: Structure of NDGA

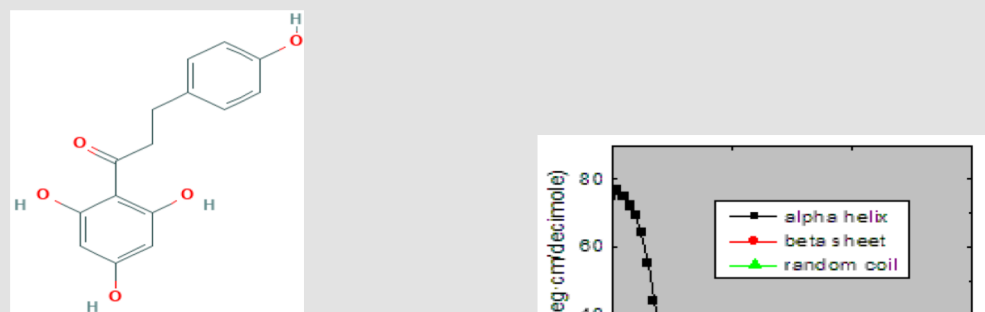


Figure 3: Structure of PHL

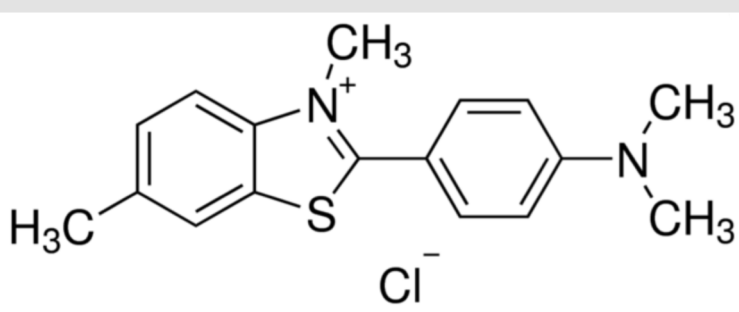


Figure 5: Thioflavin-T dye used for binding beta-amyloid complexes

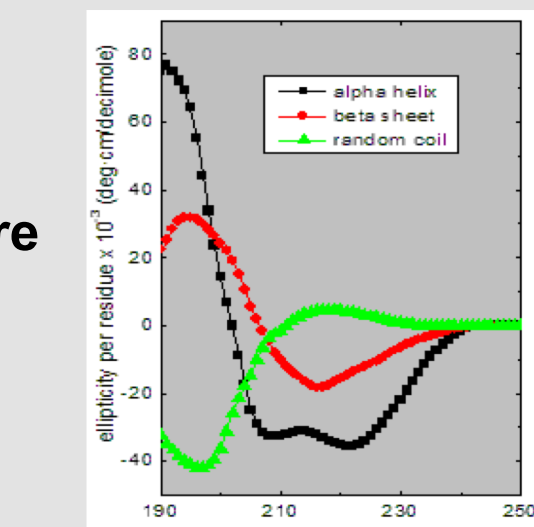


Figure 6: CD spectra of secondary structure in proteins.¹⁵

MATERIALS AND METHODS

All compounds were obtained from Sigma-Aldrich. 10 mg/mL stock solutions of GG and HEWL were prepared (4 mL each). Concentrations of 1, 2, 5, and 10 mM were then prepared for each natural inhibitor (4 mL). 2 mg/mL solutions of protein were prepared using 10 mg/mL stock protein (0.2 mL), pH 2 phosphate buffer (0.7 mL), and the respective concentration of a specific inhibitor (0.1 mL). 1 mg/mL solutions of protein were made by using 10 mg/mL stock protein (0.1 mL), pH 2 phosphate buffer (0.7 mL), and the respective concentration of a specific inhibitor (0.1 mL). pH 2 saline solution was used in place of pH 2 phosphate buffer for solutions containing HEWL as the protein to ensure favorable conditions for protein aggregation. 2 mg/mL controls were made by using 10mg/mL stock protein (0.2mL), pH 2 phosphate buffer (0.7 mL), and filter sterile water (0.1 mL). 1 mg/mL controls were made by using 10 mg/mL stock protein (0.1 mL), pH 2 phosphate buffer (0.7 mL), and filter sterile water (0.2 mL). All solutions were filter sterilized and then incubated at 60°C for 12 hours and shaking at 100 rpm. Solutions were plated in triplicate in a 96 well opaque microplate. A stock solution of ThT was created by dissolving 5 mg ThT in 5 mL pH 2 phosphate buffer. The solution was filter sterilized and was placed in each well using a multichannel pipette (0.01 mL). ThT fluorescence was monitored using a Molecular Devices SpectraMax M5 microplate reader by excitation at 440 nm and emission at 480 nm every 10 minutes for 12 hours. The CD spectrum in the far-UV region (190 - 260 nm) of a protein sample was obtained using 3 mL of solution containing 0.05 mg/mL protein using the Jasco J-815 CD spectrometer. The saline solution, acetate/phosphate buffer, PHL and EA solutions were used as controls to determine whether or not they have a high absorbance in this region of the spectrum.

RESULTS

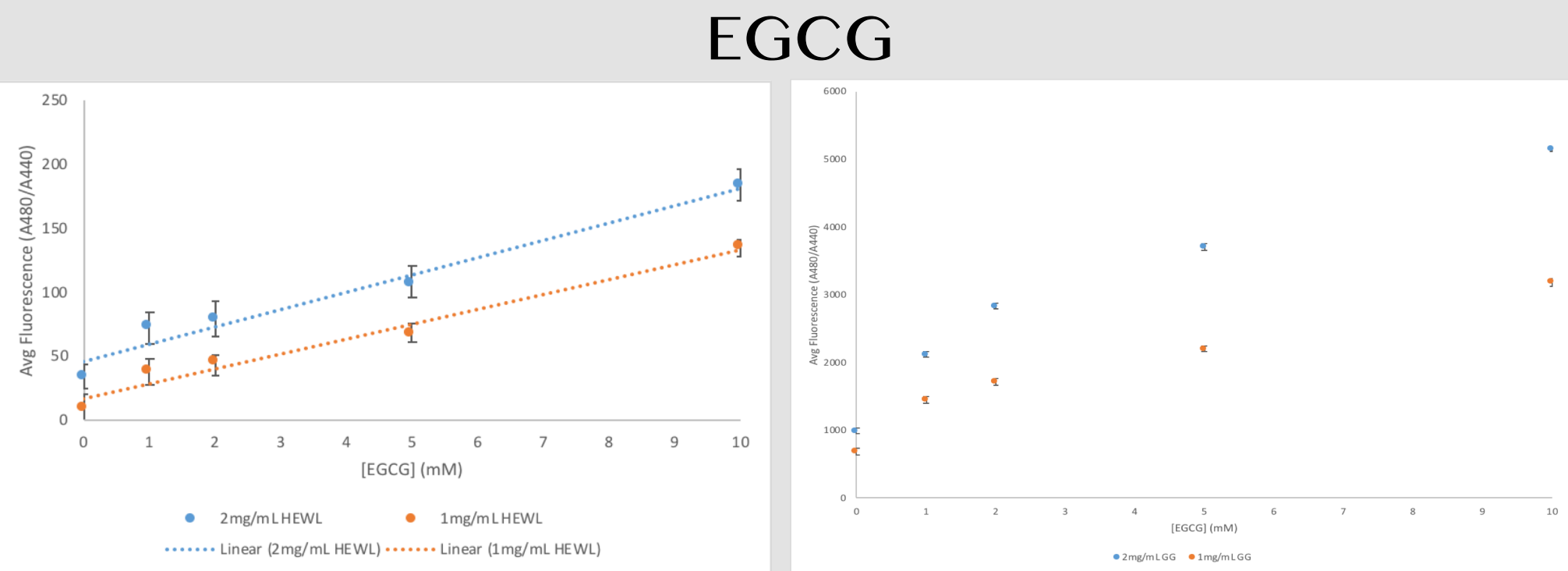


Figure 7: Dose-Dependent Response of EGCG added to HEWL. Fluorescence was averaged from one to two hours for each concentration of added inhibitor during the reading and was plotted against varying concentrations of EGCG. An increasing linear response was observed displaying a coefficient of determination of 0.9745 and 0.9679 for 1 mg/mL and 2 mg/mL HEWL, respectively. For 2 mg/mL HEWL, percent activation for 1, 2, 5, and 10 mM EGCG when compared to the control (0 mM) was 117, 134, 221, and 450%, respectively.

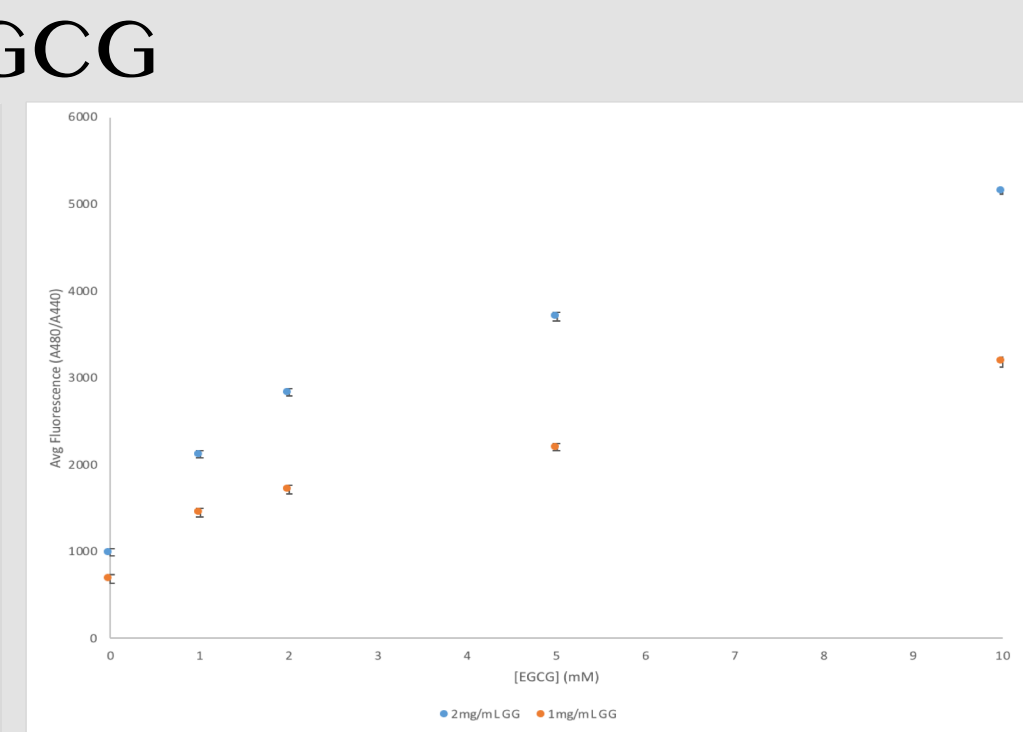


Figure 8: Dose-Dependent Response of EGCG added to GG. Fluorescence was averaged from one to two hours for each concentration of added inhibitor during the reading and was plotted against varying concentrations of EGCG. An increasing hyperbolic response was observed displaying a coefficient of determination of 0.9745 and 0.9679 for 1 mg/mL and 2 mg/mL HEWL, respectively. For 2 mg/mL HEWL, percent activation for 1, 2, 5, and 10 mM EGCG when compared to the control (0 mM) was 114, 186, 990, and 420%, respectively.

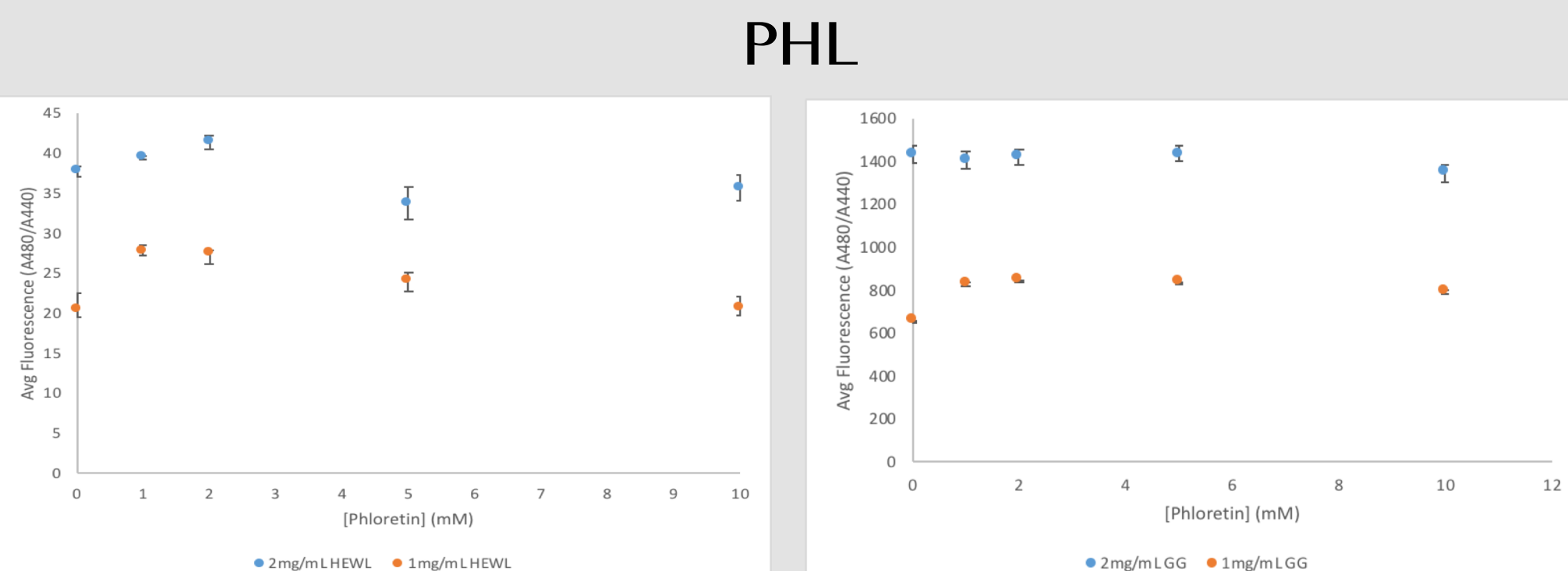


Figure 11: Dose-Dependent Response of PHL added to HEWL. Fluorescence was averaged from one to two hours for each concentration of added inhibitor during the reading and was plotted against varying concentrations of PHL. No dose-dependent responses for both 2 mg/mL and 1 mg/mL HEWL were observed.

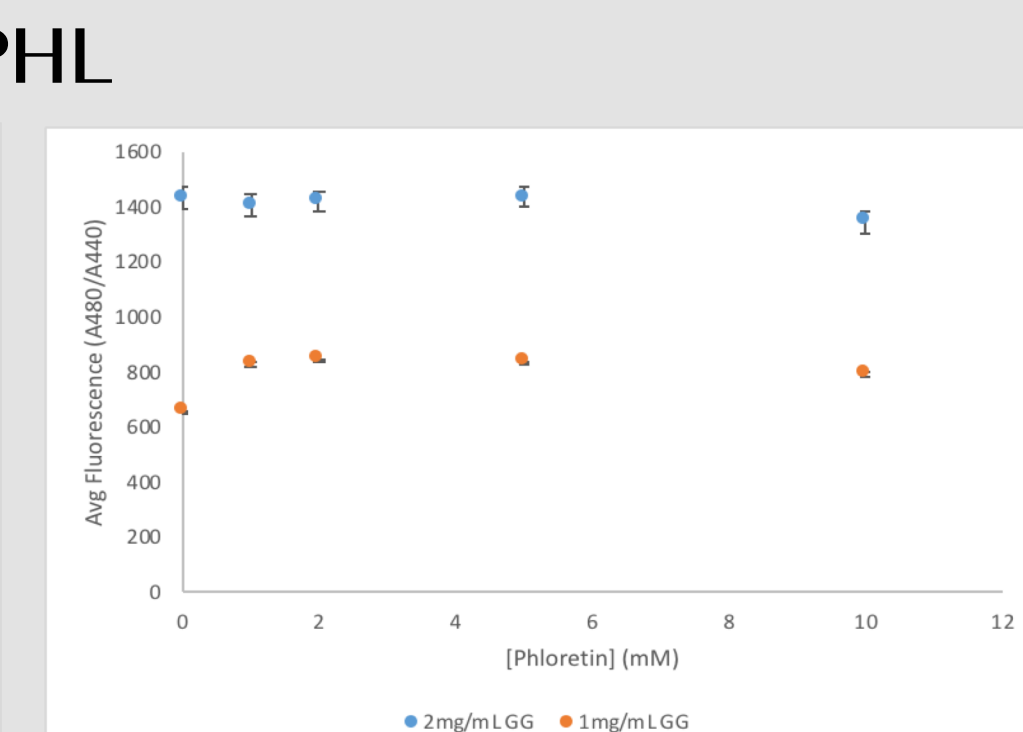


Figure 12: Dose-Dependent Response of PHL added to GG. Fluorescence was averaged from one to two hours for each concentration of added inhibitor during the reading and was plotted against varying concentrations of PHL. No dose-dependent responses for both 2 mg/mL and 1 mg/mL GG were observed.

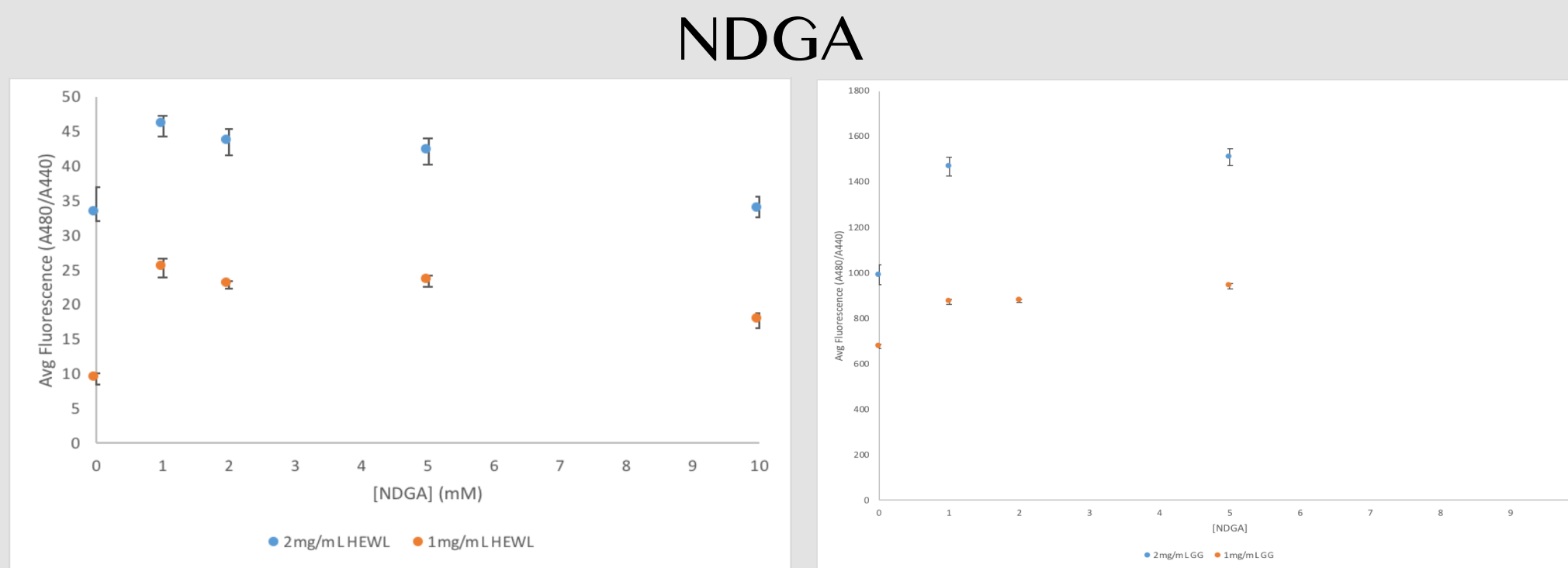


Figure 9: Dose-Dependent Response of NDGA added to HEWL. Fluorescence was averaged from one to two hours for each concentration of added inhibitor during the reading and was plotted against varying concentrations of NDGA. No dose-dependent responses for both 2 mg/mL and 1 mg/mL HEWL were observed.

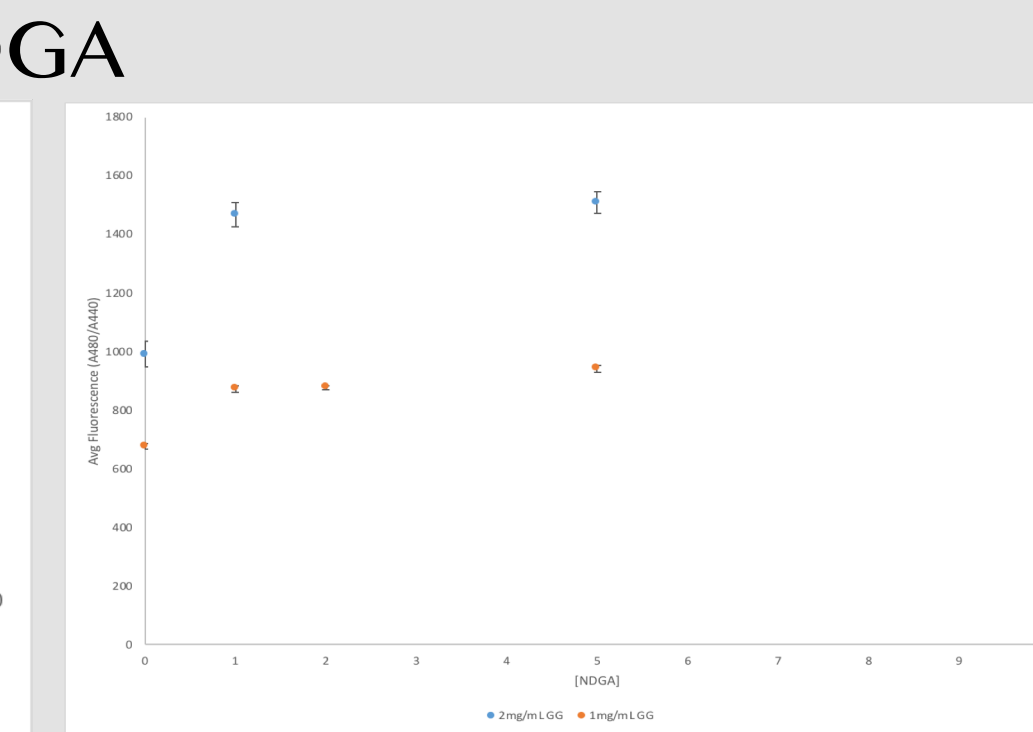


Figure 10: Dose-Dependent Response of NDGA added to GG. Fluorescence was averaged from one to two hours for each concentration of added inhibitor during the reading and was plotted against varying concentrations of NDGA. No dose-dependent responses for both 2 mg/mL and 1 mg/mL GG were observed.

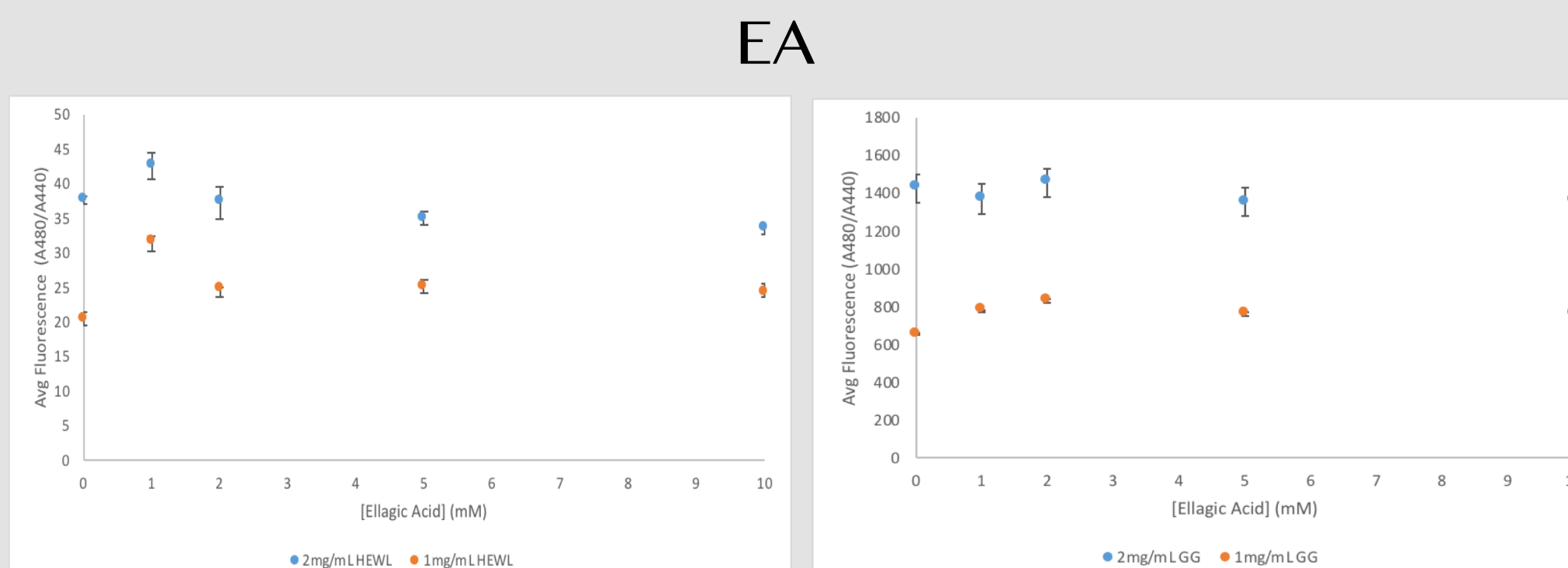


Figure 13: Dose-Dependent Response of EA added to HEWL. Fluorescence was averaged from one to two hours for each concentration of added inhibitor during the reading and was plotted against varying concentrations of EA. No dose-dependent responses for both 2 mg/mL and 1 mg/mL HEWL were observed.

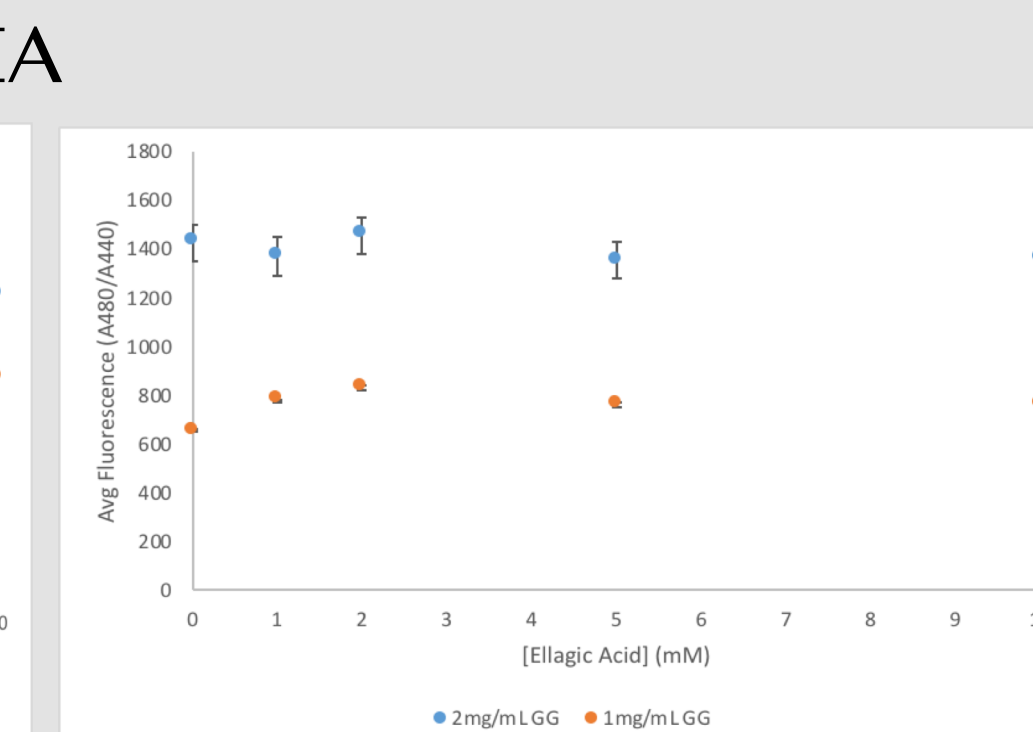


Figure 14: Dose-Dependent Response of EA added to GG. Fluorescence was averaged from one to two hours for each concentration of added inhibitor during the reading and was plotted against varying concentrations of EA. No dose-dependent responses for both 2 mg/mL and 1 mg/mL GG were observed.

CD Spectra

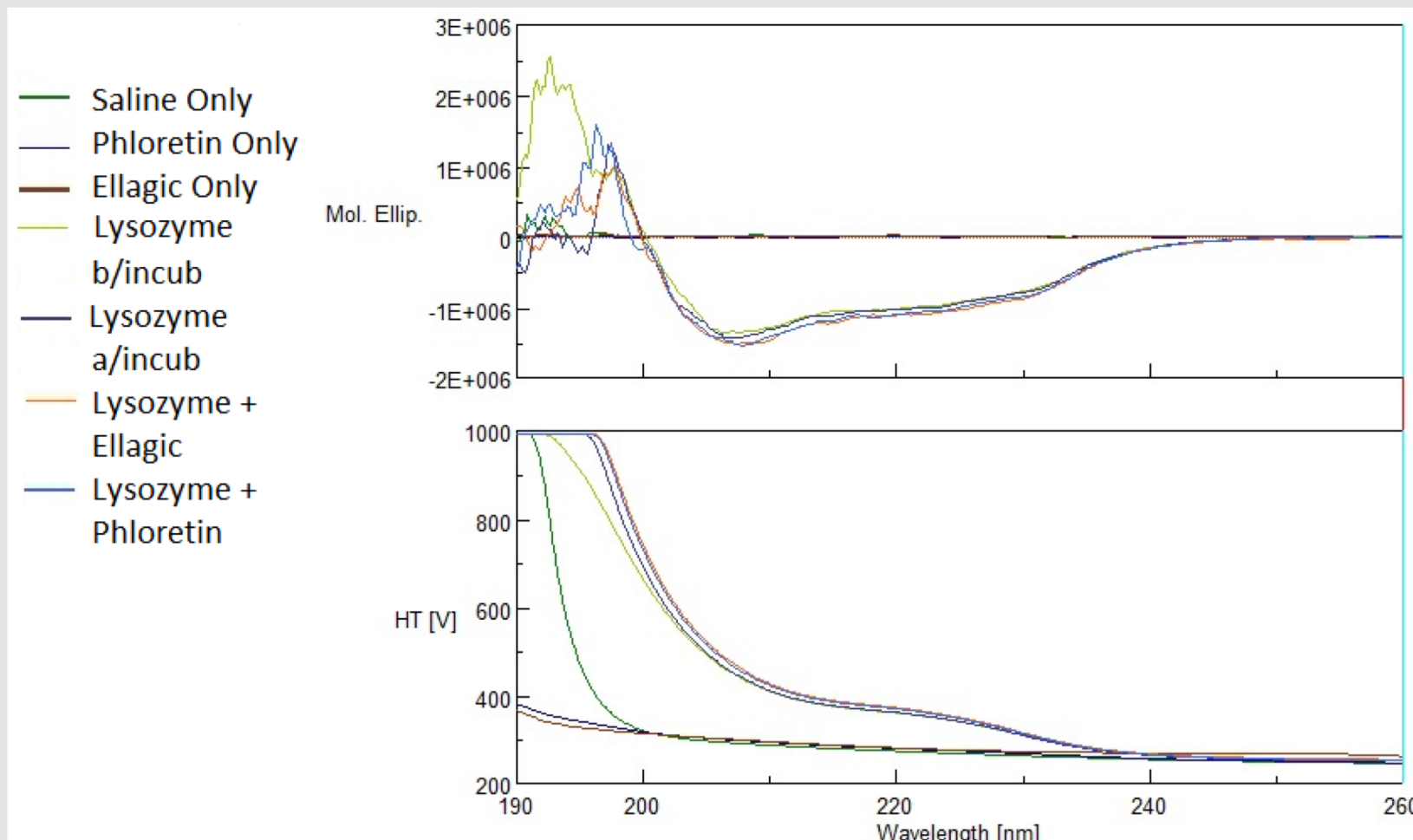


Figure 15: CD spectra for HEWL. Saline, PHL, and EA were used as controls to ensure that they are not optically active. HEWL after incubation with any inhibitor shows a positive CD band around 195 nm and two negative CD bands at 208 nm and 222 nm. Incubation in the presence of PHL and EA did not seem to change the secondary structure of HEWL.

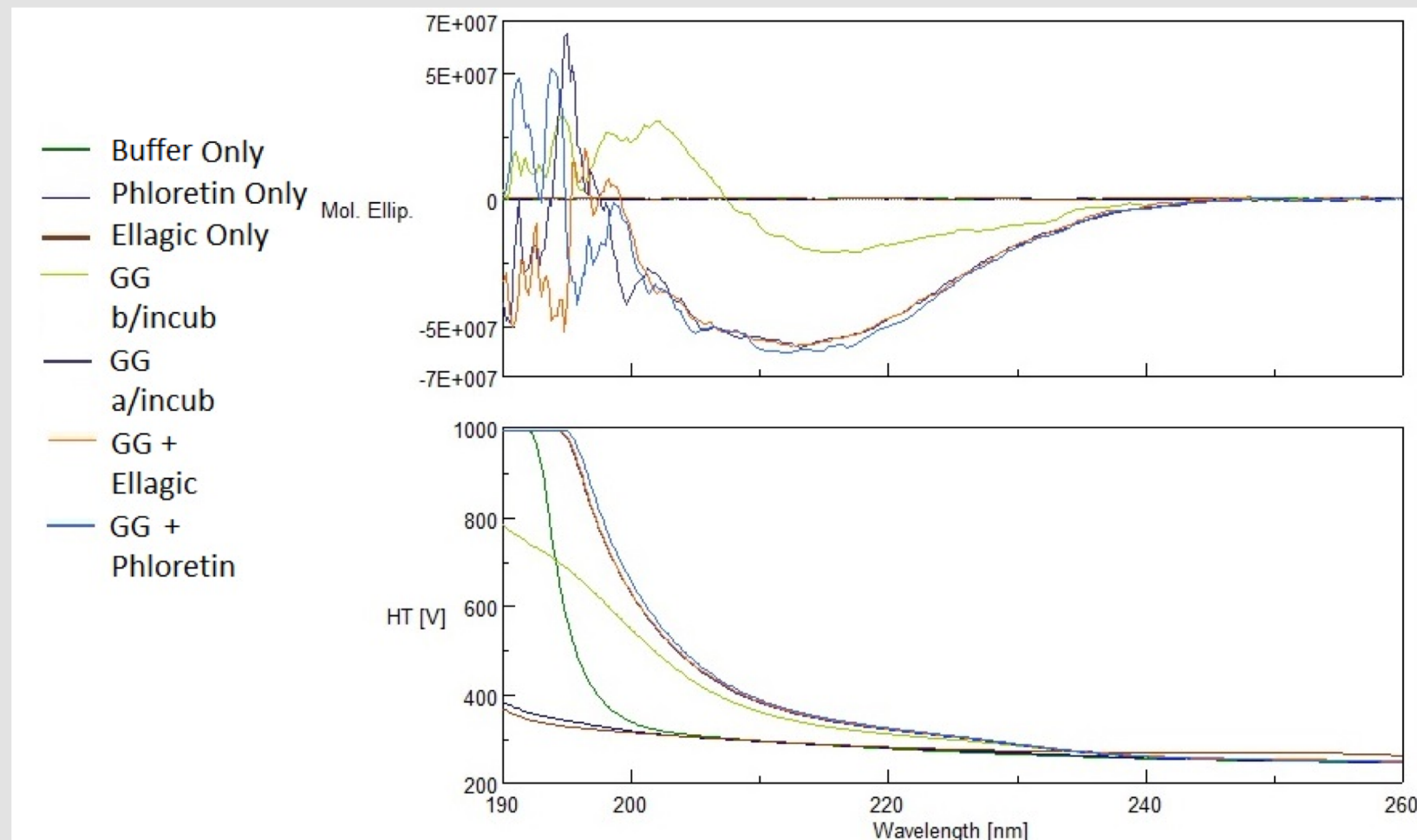


Figure 16: CD spectra for GG. Phosphate buffer, PHL, and EA were used as controls to ensure that they are not optically active. GG before incubation without any inhibitor shows a positive CD band at 218 nm and a negative CD band from 210-225 nm. After incubation, there is a decrease at 200-205 nm in GG without any inhibitor. Incubation in the presence of PHL and EA did not seem to change the secondary structure of GG when compared to the GG after incubation without any inhibitor.

DISCUSSION

Neurodegenerative diseases such as AD are of increasing concern; therefore, new ways are being explored to seek treatment or prevent certain ailments related to the formation of amyloid fibrils. This study aimed to explore the anti-amyloidogenic properties of natural polyphenols on GG and HEWL as a model system. Both GG and HEWL experienced an increasing dose-dependent response when added with EGCG. The most fluorescence was observed at the highest concentration of inhibitor. Although this is contradictory to the expected, it may result from EGCG binding to the fibril to stabilize it to increase the fluorescence intensity. Therefore, the higher the concentration of EGCG, the more fluorescence (Figure 7). The relationship between fluorescence and EGCG concentration in HEWL is linear with a coefficient of determination 0.9745 and 0.9679 for 1 mg/mL and 2 mg/mL HEWL with EGCG, respectively (Figure 7). GG experience a hyperbolic relationship, but still maintained an increasing dose-dependent response for EGCG (Figure 8). In 2 mg/mL GG, percent activation for 1, 2, 5, and 1 0mM EGCG when compared to the control (0 mM) was 114, 186, 990, and 420%, respectively (Figure 8). For 2 mg/mL HEWL, percent activation for 1, 2, 5, and 10 mM EGCG when compared to the control (0 mM) was 117, 134, 221, and 450%, respectively (Figure 6). This further demonstrates that EGCG activates the fibrils more than the control. Even though it is observed that EGCG binds to the fibril, it also conveys EGCG toxicity. With increased amounts of EGCG, some studies have seen hepatotoxicity in mice with too much oral intake.¹⁶ Since native GG is comprised of primarily beta sheets, it was noted that ThT fluorescence was more readily increased than that of HEWL which is comprised more of alpha helices than beta sheets. ThT binds to amyloid and gives a stronger fluorescence signal. Therefore, fluorescence was noted to be less for HEWL than for GG as the average fluorescence for the first two hours of analysis for the control 2 mg/mL HEWL was 33.23 and was 989.52 for 2 mg/mL GG under the same conditions after 12 hours of incubation (Figures 7 and 8). There was no dose-dependent relationship noted for NDGA, PHL, and EA in both HEWL and GG (Figures 9-14). All varying concentrations gave the same signal indicating that there was no relationship. NDGA is known to directly bind to amyloid fibril but does not appear to stabilize amyloid. PHL and EA are not directly involved in binding to the fibrils to inhibit fibril formation—they are just involved in the pathway of fibril formation and degradation. Therefore, if PHL and EA cannot bind to the formed fibrils, they will have no effect on the signal like what was observed in EGCG. Circular dichroism (CD) data was used to show the composition of secondary structure in GG and HEWL. HEWL after incubation without any inhibitor shows a positive CD band around 195 nm and two negative CD bands at 208 nm and 222 nm (Figure 15). This is indicative of alpha helical secondary structure. The presence of PHL and EA did not seem to affect the secondary structure. GG before incubation without any inhibitor shows a positive CD band at 218 nm and a negative CD band from 210-225 nm. After incubation, there is a decrease at 200-205 nm in GG without any inhibitor (Figure 16). This indicates that most of GG's native secondary structure has unfolded and changed to random coil structure. The presence of PHL and EA during incubation did not affect the secondary structure of GG as well. It would be suggested to perform CD data at a lower concentration of 0.01 mg/mL to reduce the noise seen in the 190-200 nm region of both spectra. However, there were still beta sheets formed in both HEWL and GG because ThT was able to bind and produce a fluorescence signal indicating the formation process of amyloid is kinetically a very slow process and 12 hours of incubation was not sufficient to convert most of native proteins to amyloid.

CONCLUSION

This study determined the effects of polyphenols on formation of amyloid fibrils. EGCG showed an unexpected increase in the ThT fluorescence when plotted against increasing concentrations of EGCG. This dose-dependent response was observed in both GG and HEWL perhaps because EGCG is able to bind to the formed fibril and stabilize the structure. NDGA, PHL, and EA showed no interaction with the formed fibrils in both GG and HEWL. ThT fluorescence was higher for GG than it did for HEWL because of the higher beta sheet content in its secondary structure in GG appeared to accelerate the amyloid formation. CD spectrometry showed GG's structure to have changed to random coil and HEWL structure to remain predominantly alpha helical. Longer incubation at pH 2 would be recommended to form more beta-amyloid structures. Running the CD spectra with a concentration of protein at 0.01 mg/mL would also be recommended to reduce the noise seen in the spectra. Future studies should further test other common polyphenols that are known to bind directly to formed amyloid or prevent the formation by binding to intermediates. CD spectrometry of protein incubated in the presence of EGCG would be highly recommended as well.

ACKNOWLEDGEMENTS

A special thanks to Winona State University for supporting and funding this research with the Winona State Student Research Grant and making this all possible. An additional thanks to all other assistance from other WSU students, faculty, and the chemistry department.

REFERENCES

1. Fändrich, M. Oligomeric Intermediates in Amyloid Formation: Structure Determination and Mechanisms of Toxicity. *Journal of Molecular Biology*. 2012; 421(4-5): 427-440.
2. Chiti, Dobson. Protein misfolding, functional amyloid, and human disease. *Annu Rev Biochem*. 2006; 75:333–366.
3. Xu S. Cross- β -Sheet Structure in Amyloid Fiber Formation. *J Phys Chem B*. 2009 Sep 17;113(37):12447-55. doi: 10.1021/jp903106x.
4. Caughey, Lansbury PT. Protofibrils, pores, fibrils, and neurodegeneration: Separating the responsible protein aggregates from the innocent bystanders. *Annu Rev Neurosci*. 2003;26:267–298.
5. Popovych N, Brendler JR, Soong R, Vivekanandan S, Hartman K, Basur V, et al. Site specific interaction of the polyphenol EGCG with the SEVI amyloid precursor peptide PAP(248–286). *J Phys Chem B*. 2012;116(11):3650–3658.
6. Ehrnhoefer D, Duenwald M, Markovic P, Wacker J, Engemann S, Roark M, Legleiter J, Marsh J, Thompson L, Lindquist S, Muchowski P, Wanker E. Green tea (–)-epigallocatechin-gallate modulates early events in huntingtin misfolding and reduces toxicity in Huntington's disease models. *Hum Mol Genet*. 2006; 15(18):2743–2751. doi: 10.1093/hmg/ddi210.
7. Pallano F, Lee J, Grimsler N, Kelly J. Toward the molecular mechanism(s) by which EGCG treatment remodels mature Amyloid Fibrils. *J Am Chem Soc*. 2013;135(20):7503–7510.
8. Ono K, Hasegawa K, et al. Nordihydroguaiaric acid potentially breaks down pre-formed Alzheimer's β -amyloid fibrils *in vitro*. *Journal of Neurochemistry*. 2002; 81(3):434-40.
9. Terzi E, Hölzemann G, Seelig J. *J Mol Biol*. 1995;252:633–642.
10. Seelig J, Lehmann R, Terzi E. *Mol Membr Biol*. 1995;12:51–57.
11. Jo E, Boggs J M. *Biochim Biophys Acta*. 1994;1195:245–251.
12. Zhong L, Liu H, et al. Ellagic acid ameliorates learning and memory impairment in APP/PS1 transgenic mice via inhibition of β -amyloid production and tau hyperphosphorylation. 2018; 16(6):4951–4958.
13. Kiasalari Z, Heydariard R, et al. Ellagic acid ameliorates learning and memory deficits in a rat model of Alzheimer's disease: an exploration of underlying mechanisms. *Psychopharmacology*. 2017; 234(12):1841-1852.
14. E. Takai et al. Scanning Electron Microscope Imaging of Amyloid Fibrils. *American Journal of Biochemistry and Biotechnology*. 2014; doi: 10.3844/ajbbbsp.2014.31.39.
15. KBI Biopharma—Alliance Protein Laboratories. Circular Dichroism (CD). 2018. Accessed April 6, 2019. <https://www.ap-lab.com/circular-dichroism>
16. Lambert J, Kennett M, Sang S, et al. Hepatotoxicity of High Oral Dose (–)-Epigallocatechin-3-Gallate in Mice. *Food Chem Toxicol*. 2010; 48(1):409-416.